geosciences

MDPI

Article

Inventory of Landslides in the Northern Half of the Taihang Mountain Range, China

Xuewei Zhang [1,2], Chong Xu [2,3,*], Lei Li [4], Liye Feng [1,2] and Wentao Yang [1]

[1] School of Soil and Water Conservation, Beijing Forestry University, Beijing 100083, China; zxw98331@bjfu.edu.cn (X.Z.); yang_wentao@bjfu.edu.cn (W.Y.)
[2] National Institute of Natural Hazards, Ministry of Emergency Management of China, Beijing 100085, China
[3] Key Laboratory of Compound and Chained Natural Hazards Dynamics, Ministry of Emergency Management of China, Beijing 100085, China
[4] Institute of Geology and Geophysics, Chinese Academy of Sciences, Beijing 100029, China; lilei232@mails.ucas.ac.cn
* Correspondence: xc11111111@126.com or chongxu@ninhm.ac.cn

Abstract: The Taihang Mountains are a critical mountain range and geographical boundary in eastern China. Landslide disasters are particularly common in this region and usually cause serious casualties and property damage. However, previous landslide inventories in the region are limited and lack comprehensive landslide cataloguing. To address this gap, the northern half of the Taihang Mountain Range was selected for this study. A landslide database for the area was constructed using multi-temporal high-resolution optical imagery from the Google Earth and human–computer interactive visual interpretation technology. The results indicate that at least 8349 landslides have occurred in the Taihang Mountain Range, with a total landslide area of about 151.61 km^2. The size of the landslides varies, averaging about 18,159.23 m^2, with the largest landslide covering 2.83 km^2 and the smallest landslide only 5.95 m^2. The significance of this study lies in its ability to enhance our understanding of the distribution of landslides in the northern half of the Taihang Mountains. Furthermore, it offers valuable data references and supports for landslide assessment, early warning systems, disaster management, and ecological protection efforts.

Keywords: northern half of the Taihang Mountain Range; landslide database; human–computer interactive visual interpretation

Citation: Zhang, X.; Xu, C.; Li, L.; Feng, L.; Yang, W. Inventory of Landslides in the Northern Half of the Taihang Mountain Range, China. *Geosciences* **2024**, *14*, 74. https://doi.org/10.3390/geosciences14030074

Academic Editors: Samuele Segoni and Jesus Martinez-Frias

Received: 27 January 2024
Revised: 1 March 2024
Accepted: 7 March 2024
Published: 10 March 2024

1. Introduction

Landslides are one of the major types of geologic hazards globally, causing severe casualties and property damage every year [1–4]. How to prevent and mitigate landslide disaster risk losses has long been a focus of research. Landslide databases are a valuable source of information for studying landslides [5]. Not only do they play a pivotal role in comprehending the intricacies of landslide causes, types, and processes, but they also assume significance in characterizing the spatial distribution patterns and assessment of landslides. For example, Cui et al. (2023) [6] focused on the Syntaxis region in the western Himalaya and developed a comprehensive landslide database comprising 7947 landslides. They then identified 9 key factors for landslide hazard assessment, analyzed the spatial distribution pattern of landslides, and assessed the landslide risk in the study area. These findings are significant for disaster risk reduction and land use planning efforts in similar areas.

Many countries and regions have now completed landslide inventories that are comprehensive and well-designed, providing detailed information on the content and structure of landslides. Mirus et al. (2020) [7] compiled existing publicly available landslide inventories and created a comprehensive map of landslides in the United States. The European landslide database proposed by Van and Hervás (2012) [8] analyzes landslide databases

in 22 countries and regional landslide databases in 6 countries, with a total of about 633,700 landslides. Fausto Guzzetti (2000) [9] created a database of landslides that occurred in Italy between 1279 and 1999. Brenda Rosser et al. (2017) [10] describe the development of the New Zealand Landslide Database, which currently contains 22,575 landslide records. Japan, being an earthquake-prone country, experiences earthquakes that can trigger massive landslides. On 6 September 2018, an Mw 6.6 earthquake struck Hokkaido, Japan, and Cui et al. (2021) [11] constructed a co-seismic landslide inventory for this event, recording a total of 12,586 landslides.

China's complex geology and varied topography make it prone to landslides. Xu et al. (2020) [12] investigated about 80,000 landslides in the Loess Plateau using high-resolution satellite images. Zhao et al. (2023) [13] identified 1073 landslides along the western part of the Sichuan–Tibet Engineering Corridor through remote sensing interpretation and conducted a two-month field survey for validation. Zhang et al. (2022) [14] investigated large-scale landslides in the city of Lvliang on the eastern Loess Plateau and found 12,110 landslides. Li et al. (2022) [15] completed the cataloging of large (area > 5000 m^2) landslides in Baoji City, Shaanxi Province, by visual interpretation, identifying a total of 3422 landslides with a total area of 360.7 km^2. Although China has carried out landslide research in many areas and made significant progress, research on landslides in mountain ranges is still relatively weak.

The northern half of the Taihang Mountain Range, as a magnificent mountain range developed within the ancient Craton, has continuously recorded more than 2.5 billion years of geological evolution [16]. The area is characterized by complex geological conditions and a variety of climatic types, making it a typical landslide occurrence area. Landslide disasters occur frequently, seriously threatening the lives and properties of local people. Previous studies have mainly focused on localized geohazards in various scenic spots, and relatively few landslides have been interpreted on a large scale and in an all-round way in the mountain range. In order to fill this gap, this study completed the visual interpretation of landslides in the region based on high-resolution satellite images from the Google Earth platform. The established detailed and complete landslide database in the northern half of the Taihang Mountain Range can provide data support and reference for disaster prevention and mitigation work in the region.

2. Study Area

The Taihang Mountain Range serves as the watershed between the second and third terraces in China, forming a natural divide between the Loess Plateau and the North China Plain. Its geographical position is of immense significance. The range is divided into northern and southern halves, demarcated by the 38° N boundary. The northern half of the Taihang Mountains is bordered by the Bohai Bay Basin to the east, the Fenwei Graben System, the Lvliang Mountains and the Ordos Basin to the west, and the Yanshan Fold Belt to the north [16]. The entire study area spans Beijing, Shanxi province, and Hebei province, encompassing a geographic range of 38.0° N to 40.36° N and 112.69° E to 116.26° E (Figure 1). With an overall area of approximately 33,000 km^2, the study area has a varied topography with high mountains in the north and low mountains in the south. This particular region is also home to the Wutai Mountain, which boasts a peak altitude of 3061 m, making it the highest point in the area. Notably, numerous rivers traverse this landscape, including the Yongding River, Juma River, Tang River, Sha River, and Hutuo River [17]. These waterways carve out impressive gorge landscapes as they traverse through the mountains, eventually converging into the Haihe River system. In terms of geotectonic position, the northern half of the Taihang Mountains is located in the middle of the North China Plate. Rock layers widely distributed throughout this region are primarily made up of quartz sandstone from the Great Wall System of the Middle Paleozoic era. The tectonic activities associated with the Taihang Mountains fault zone have significantly influenced the uplift of mountain ranges and the subsidence of the North China Basin [18]. In the Cenozoic Era, the present Roach Rock landform was formed after a

number of uplift and flattening processes. In terms of climate type, the northern half of the Taihang Mountain Range falls within the temperate continental monsoon climate. This region experiences distinct seasonal variations, with average annual temperatures hovering around 10 °C. This region experiences sweltering summers, as well as chilly winters, with the majority of precipitation concentrated in July and August. The landscape and climate have jointly contributed to its ecological richness and natural beauty. Extensive historical records indicate that during periods of extreme rainfall in July 1996, August 2016, and July 2021, a significant number of geologic hazards materialized in the area. According to the China Seismic Network, the northern half of the Taihang Mountains and its surrounding environs have been struck by earthquakes of magnitude 5.0 to 6.0 on multiple occasions throughout history, with eleven significant earthquakes of magnitude 7.0 or higher having occurred. The high frequency and intensity of seismic activity in the region, coupled with its intricate topographic variations and hydrogeological features, increase the likelihood of landslide hazards within the region.

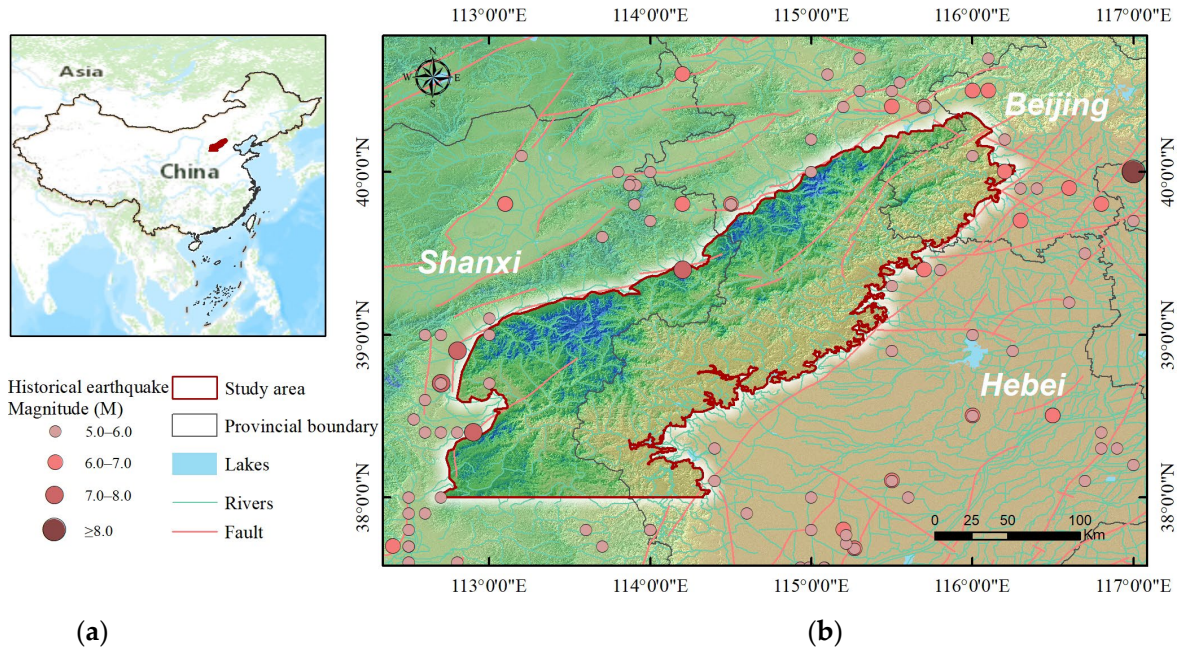

Figure 1. Overview of the study area. (**a**) Geographic location of the northern half of the Taihang Mountain Range. (**b**) Map of active ruptures, historical earthquakes, and topographic distribution in the northern half of the Taihang Mountain Range.

3. Data and Methods

3.1. Data Description

Google Earth is a virtual earth software developed by Google Inc. The satellite images of this platform, instead of being a single data source, integrate data from satellite images and aerial photography. Among them, the satellite image part and the aerial photography part are from various sources, which brings great convenience to our landslide interpretation work. In the area we focus on, the Google Earth platform can provide high-definition satellite images with a resolution of about 0.5 m, which fully meets the accuracy requirements of landslide investigation. In addition, the Google Earth platform also has a multi-temporal historical image function, which can display different satellite images of the same area in different historical periods. As shown in Figure 2, we can identify landslides more accurately by comparing satellite images from different periods. Therefore, the landslide interpretation work using Google Earth has high practicality and reliability.

Figure 2. Google Earth images of the same location (39.592° N, 115.789° E) at three different times (**A**–**C**). White dashed lines indicate landslide boundaries and arrows indicate direction.

3.2. Interpretation Methods

Currently, landslide interpretation methods have evolved from traditional visual interpretation to human–computer interactive interpretation and automatic interpretation of landslides [19,20]. Among them, visual interpretation is the most essential approach to obtain landslide information using remote sensing images. It does not require complex techniques or equipment, relying mainly on the interpreter's knowledge of the target's identification, sufficient experience, and familiarity with background information to eventually identify landslides by analyzing and judging the images using their expertise [21]. However, visual interpretation suffers from low efficiency and susceptibility to subjective factors. Human–computer interactive interpretation is a remote sensing image preprocessing method that takes the interpreter as the core and utilizes the computer as an auxiliary means, which can improve interpretation efficiency and accuracy. However, in essence, no new breakthroughs have been made, and human–computer interactive interpreting still belongs to the category of visual interpreting [22]. Remote sensing intelligent interpretation, on the other hand, is an automated process of interpreting and analyzing image content based on geoscientific knowledge and remote sensing expertise. Although automated extraction can greatly save time and labor, the method is still in the stage of further research and has not yet established a perfect theoretical system. Therefore, in this study, we choose the human–computer interactive visual interpretation method to complete the landslide interpretation work. To avoid missing areas, the study area was divided into eleven small $1^\circ \times 1^\circ$ units. Taking advantage of the fact that the 3D features of Google Earth images allow the user to zoom in on the morphological appearance of the terrain, thus revealing the advantages of subtle morphological changes, the latitude and longitude grids provided by the platform were added to perform a grid-by-grid landslide interpretation. We kept the visual elevation around 2 km and circled the boundary of the landslide by adding vector polygons (Figure 3). When a situation is encountered where the full extent of the landslide cannot be recognized, the zoom in and zoom out tools can be used to make timely adjustments.

The identification of landslides is the ability to screen remotely sensed imagery to identify the differences in spectral features and the magnitude of feature patterns between the landslide and the surrounding area [23]. Landslide identification signs can be categorized into direct and indirect signs. Directly interpreted signs refer to the extraction of information about the landslide itself, such as morphological features, color features, and structural texture features of the landslide body shown on the remote sensing image, etc. Indirectly interpreted signs are used to analyze and judge special phenomena such as geomorphology, vegetation distribution, and water patterns near the geohazard, which can serve as an important basis for the identification of landslides [24]. In this study, we mainly utilize the following types of signs to identify landslides:

- Morphological signs: The distribution of the landslide body shows an irregular step-like shape, and there are fissures in its interior, which are mainly located in the center and the leading edge; these fissures are important signs of landslide activity. The undulating terrain formed by the sediments at the leading edge of the landslide presents a tongue-like shape. In addition, the gullies formed by the development of the two sides of the landslide body show the phenomenon of homologous double gullies. It is noteworthy that the perimeter of the landslide presents a rim-chair-like structure, and this morphological change is also an important sign of landslide activity.
- Rock and soil structure signs: The rock and soil within the limits of the landslide often show signs of loosening, as well as discontinuities in the bedrock stratigraphy and production characteristics and surroundings.
- Color signs: Uneven color distribution occurs due to the destruction of vegetation and fragmentation of the surface of the landslide. Sometimes the whole landslide will have a light tone such as greyish white or greenish white.
- Vegetation signs: The vegetation texture is discontinuous, and the vegetation on the landslide body shows a pattern of sabre trees and drunken forest stands.
- Hydrological signs: Unusual bends in rivers or sudden narrowing of local channels. In addition, geological phenomena such as wetlands and springs are present on the landslide surface as well as linear outcrops of groundwater at the leading edge of the slide zone.

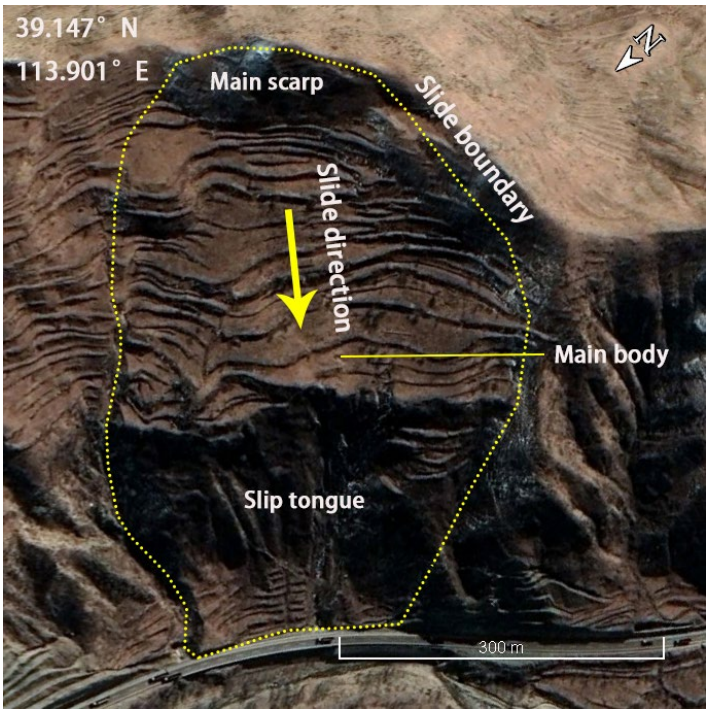

Figure 3. Example of landslide delineation.

The presence of any of the aforementioned signs can serve as a valuable indicator for identifying potential landslides. It is essential to acknowledge that the utilization of these signs is flexible and adaptable to different terrain and environmental conditions. However, there is no single combination of signs that can be applied universally in all situations [25]. To ensure the comprehensive identification of landslides, we double-checked and supplemented the results of previous interpretations during the identification process. Finally, we obtained a complete list of landslides in the northern half of the Taihang Mountain Range.

4. Results

4.1. Inventory of Landslides in the Northern Half of the Taihang Mountain Range

Based on the above methodology and landslide signatures, we completed the cataloging of landslides in the northern half of the Taihang Mountains. As shown in Figure 4, a total of 8349 landslides were identified in the study area. The 8349 landslides in the northern half of the Taihang Mountains are distributed within nine cities: Datong, Xinzhou, Yangquan, Taiyuan, and Jinzhong in Shanxi Province, Zhangjiakou, Baoding, Shijiazhuang in Hebei Province, and Beijing.

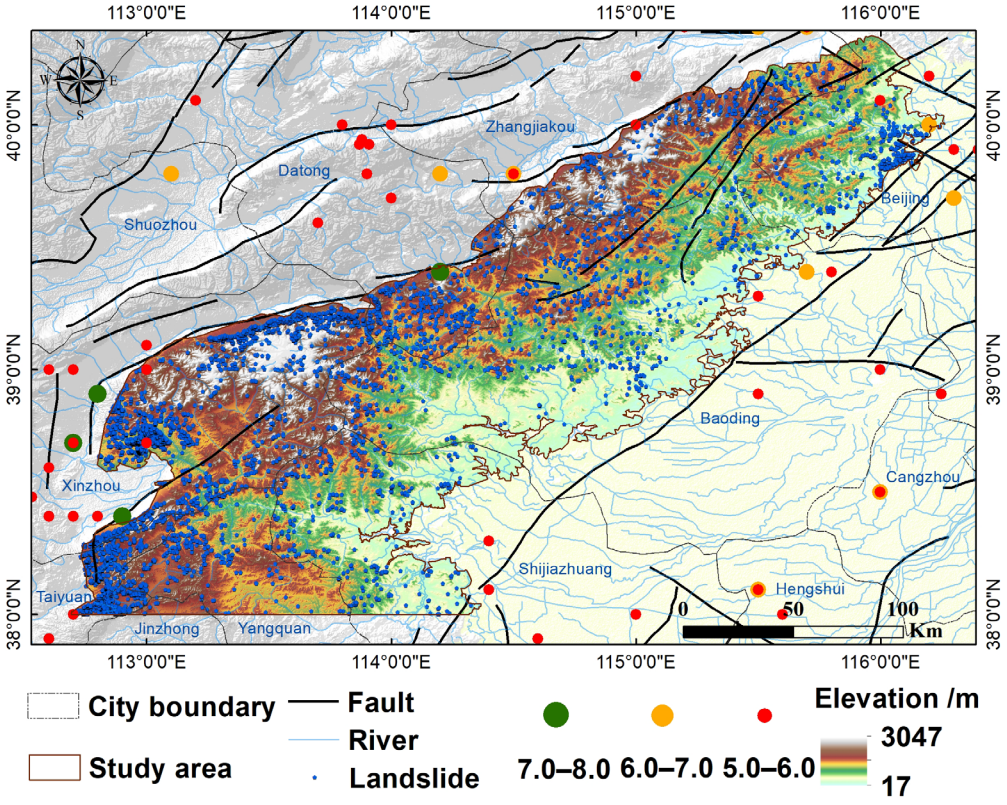

Figure 4. Distribution of landslides in the northern half of the Taihang Mountain Range.

From the landslide distribution map (Figure 4) and point density map (Figure 5), it can be seen that the landslides are mainly distributed in four regions, namely, the Fanshi-Lingqiu area, the Yuanping-Wutai area, the Dingxiang-Yangqu-Yuxian area in Shanxi Province, and the Mentougou area in Beijing. With a search radius of 5000 m, the density of landslide distribution was up to 24.62 km^{-2}. Overlaying the distribution of seismic points shows that there is a correlation between landslide point density and seismic points. Landslides develop densely in areas with a high distribution of seismic sites; for example, the Taihang Mountains around Taiyuan and Xinzhou are a highly landslide-prone area, and there have been many earthquakes near the area, four of which have been of magnitude 7 or higher.

Statistics on the area of single landslides in the northern half of the Taihang Mountains showed that the cumulative area of landslides was 151.61 km^2, with an average area of 18,159.23 m^2. The largest landslide area was 2.83 km^2, located in Fangshan District, Beijing (39.664° N, 115.784° E), where the landslide included three villages. The smallest landslide area was 5.95 m^2. There were 744 landslides smaller than 103 m^2, 4208 landslides of 10^3–10^4 m^2, 3204 landslides of 10^4–10^5 m^2, and only 193 landslides larger than 10^5 m^2, occupying 8.91%, 50.40%, 38.38%, and 2.31% of the total number of landslides, respectively. The cumulative frequency curve reflects the trend of relative frequency of landslide area values from 0–100% (Figure 6). It can be seen from the curve that landslides with landslide

areas between 10^3–10^4 are the most prominent, which is consistent with the statistical results of the values.

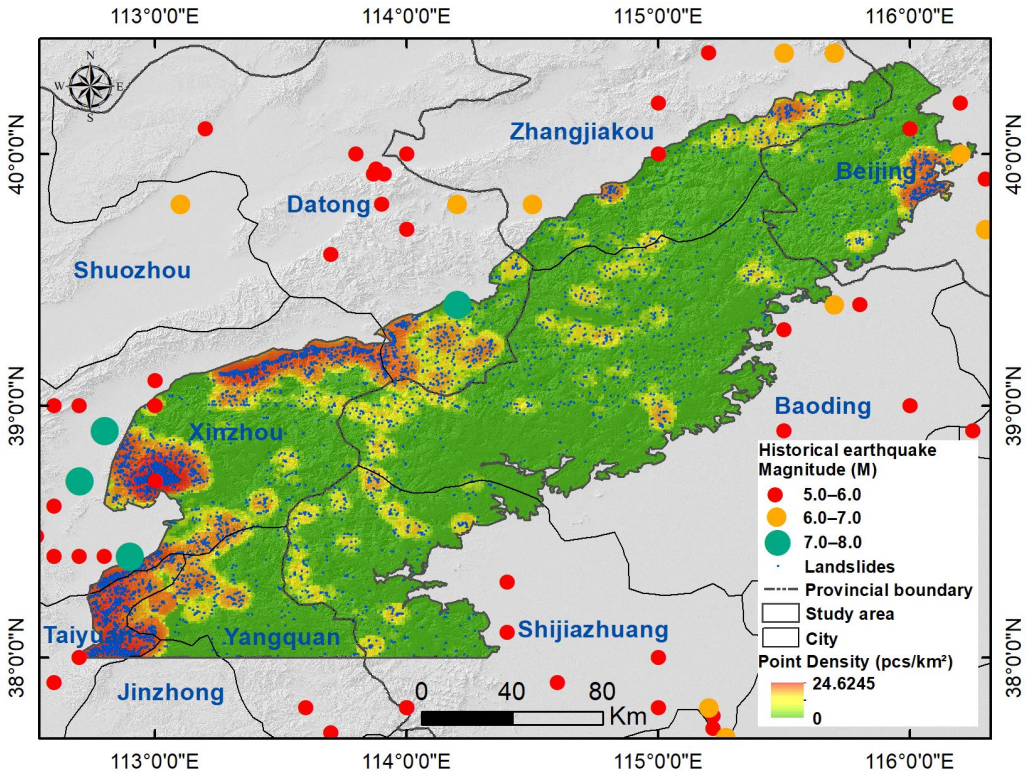

Figure 5. Map of landslide point density in the northern half of the Taihang Mountain Range.

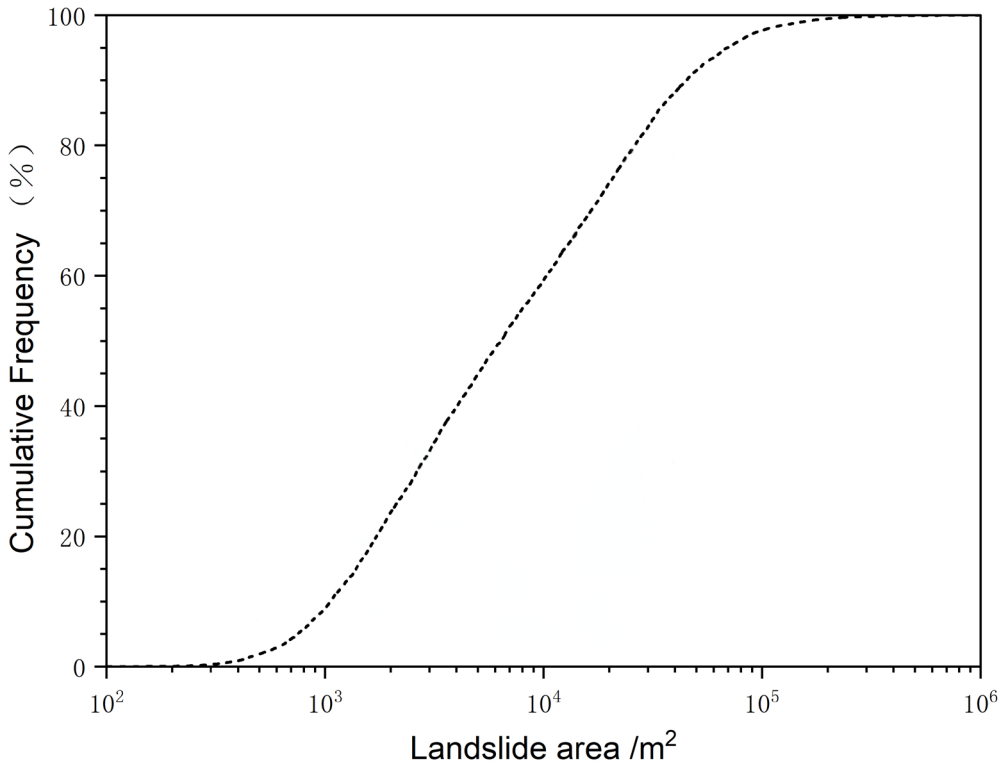

Figure 6. Area vs. cumulative frequency of landslides in the northern half of the Taihang Mountains.

4.2. Demonstration of Typical Landslides

As shown in Figure 7, we chose nine single landslides with typical characteristics arranged from north to south to visualize the distribution and morphology of the landslides more intuitively. With these pictures, it can be observed that the slope geotechnical body starts to slide along the through shear toward the critical surface. These landslides exhibit distinctive features, such as the morphology of the landslide body, the backscarp of the landslide, the landslide boundary, the direction of movement, and the buildup of the landslide.

Figure 7. Display of typical landslides in the northern half of the Taihang Mountain Range. The dash lines represent the slide boundary; The arrows represent the slide direction.

Influenced by a variety of factors such as regional tectonic and climatic environment, landslides are densely developed in the Taihang Mountains within Shanxi. Figures 8 and 9

show the landslide patterns in the localized areas of the Fanshi-Lingqiu landslide area and the Yuanping-Wutai landslide area, located at 39.199° N, 113.559° E and 38.726° N, 113.023° E, respectively. These landslides show band and cluster distribution in space. The study of these landslide clusters can provide a deeper understanding of the formation and evolution of landslides in the northern half of the Taihang Mountains and is also of great significance in promoting the development of geosciences.

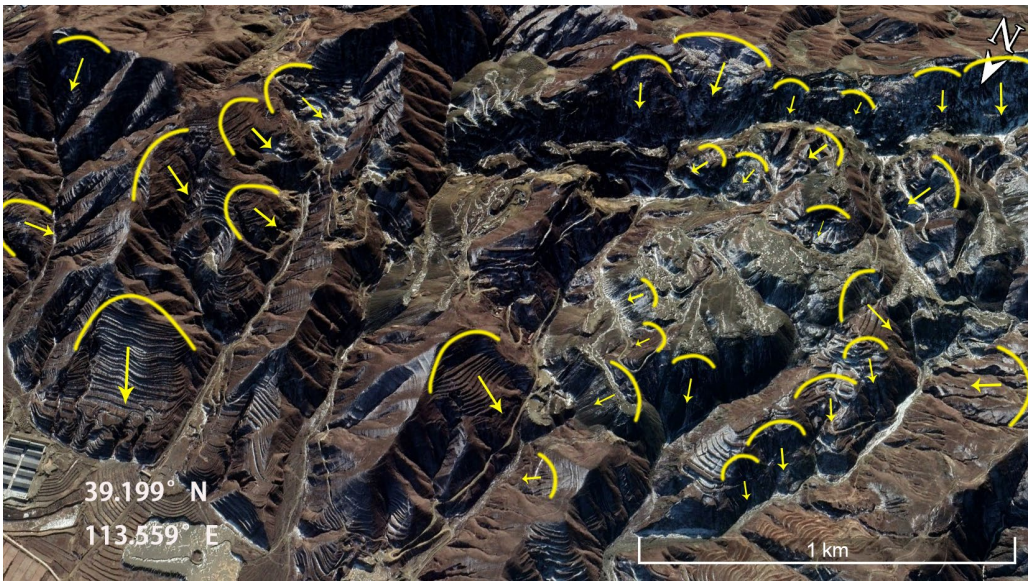

Figure 8. Typical landslide area in Fanshi County (localized). The yellow lines represent the slide boundary; The arrows represent the slide direction.

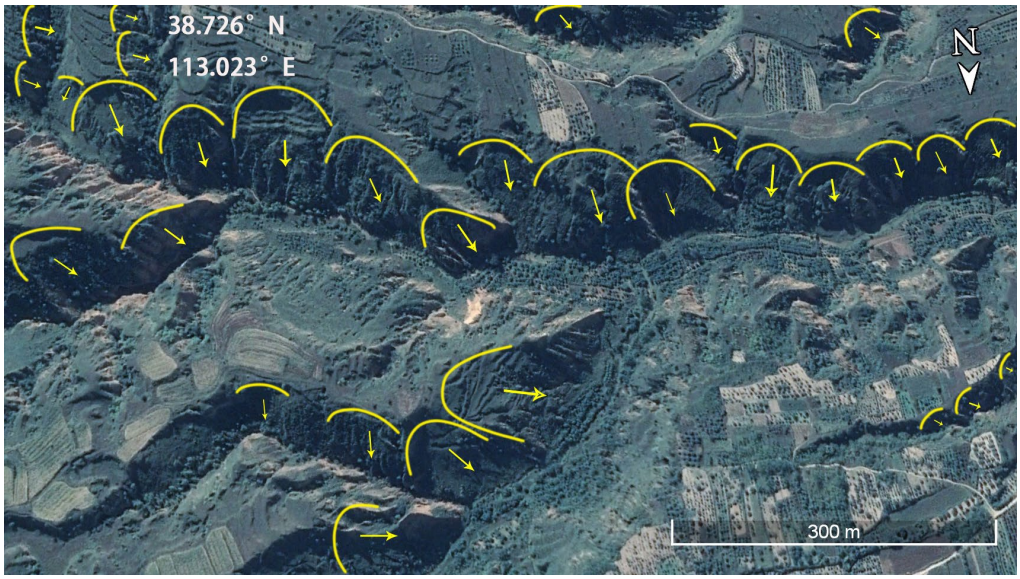

Figure 9. Typical landslide area in Yuanping City (localized). The yellow lines represent the slide boundary; The arrows represent the slide direction.

5. Discussion

Landslides in a broad sense include all forms of slope material movement, such as landslide in the narrow sense, avalanches, debris flows, and mudflows, etc. [26,27]. Mountains cover about 27% of the world's surface and directly support 22% of the global population, and in the event of a landslide, the damage and impact would be even greater [28]. Globally, landslides occur with a wide geographical distribution and varying frequency of

occurrence. From the tropics to the frigid zone, from mountains to plains, landslides can occur. However, due to differences in geological, climatic, and ecological characteristics, the frequency and magnitude of landslides vary widely from region to region [29]. For example, the United States is a mountainous country, especially in the west. Landslides occur mainly during seasons of abundant rainfall, especially in spring and winter. In addition, seismic activity is an important factor in triggering landslides. Japan is an island country located on the Pacific Rim Seismic Zone, where earthquakes and rainfall are very frequent. Landslide hazards in Japan are also influenced by its unique mountainous and hilly terrain. Many areas in Italy are also threatened by landslides [30]. In areas such as the Alps and the Apennines, rainfall and snowmelt are the main factors contributing to landslides. As an important mountain range in China, the Taihang Mountains have their own unique characteristics, and these characteristics are reflected in landslide dynamics. First, from the geological features, the Taihang Mountains are located at the junction of the North China Plate and the South China Plate, with a complex geological structure and the development of faults, folds, and other geological structures. This complex geological background makes landslides occur more frequently in the Taihang Mountains. Second, climatic factors are also important factors affecting landslide dynamics in the Taihang Mountains. Rainfall in the Taihang Mountains is mainly concentrated in the summer, and the intensity of rainfall is high. This climate is more likely to increase the risk of landslides. In addition, the ecological characteristics of the Taihang Mountains are very unique and rich. It is a habitat for many wildlife species and is home to a wide range of plant species and rare animals. Together, these resources form a unique and fragile ecosystem in the Taihang Mountains. Therefore, it is of great significance to study landslides in the Taihang Mountains.

5.1. Comparison with the Existing Database of Landslides in the Taihang Mountains Region

The creation of a landslide database helps to provide a clearer understanding of landslide distribution patterns and facilitates landslide evaluation. In recent years, many scholars have studied the landslide inventory in the Taihang Mountain region, as shown in Table 1. Ma et al. [31] carried out a detailed geohazard investigation of Qinglongxia Scenic Spot in the South Taihang Mountainous Area located in Huguan County, Shanxi Province, and identified 17 landslides and 52 collapses. This study is of great significance to the planning, construction, and safety management of mountain and canyon-type scenic spots. Wu et al. [32] used a combination of aerial map interpretation, terrain analysis, field survey and climate monitoring to analyze the talus slope activity in the Xiaowutai Mountain National Nature Reserve in the North Taihang region of China, and 213 sites were interpreted, with a study area of 71.54 km^2. Li et al. [33] investigated 40 landslides triggered by an extreme rainstorm on 21 July 2012 in Sancha Village, Fangshan District, Beijing, China. Wei et al. [34] investigated Laiyuan County located in the northern part of the Taihang Mountains, which covers an area of about 2448 km^2 with a total of 94 landslides. A landslide susceptibility map was drawn based on the landslide data, which provided a reference for reducing landslide risk and planning land use. Zhang et al. [35] conducted a survey of geologic hazards in Xindu District, Xingtai City, in the eastern foothills of the southern section of the Taihang Mountain Range, and found a total of 102 landslides, 84 collapses, and 5 mudslides in the area, which helped to study the characteristics and distribution patterns of geologic hazards. Gao [36] analyzed the field survey and indoor remote sensing images of the Bailey Gorge area of the Reject River at the northern end of the Taihang Mountains and finally came up with 195 avalanche rockfalls, and an in-depth study of these data resulted in a hazard assessment map of avalanche rockfalls in the Bailey Gorge area. Lv et al. [37] identified 318 avalanches developed in the Taihang Mountain Grand Canyon in the South Taihang Mountain area within the territory of Huguan County, Shanxi Province, dominated by high-level small rocky avalanches. The research results can provide a reference for geologic disaster prevention and mitigation in the high mountain canyon area.

Table 1. Inventory of landslides in the Taihang Mountain Range.

No.	Location	Landslide Number	Landslide Area (km^2)	Source
1	Qinglong Gorge Scenic Area	69	/	[31]
2	Xiaowutai Mountain National Nature Reserve	213	71.54	[32]
3	Sancha village, Fangshan District	40	/	[33]
4	Laiyuan county, Hebei Province	94	2448	[34]
5	Xindu district, Hebei Province	191	1941	[35]
6	Bailixia, Junma river region	195	/	[36]
7	Taihang Mountain Grand Canyon	318	/	[37]
8	The northern half of the Taihang Mountains region	8349	33,000	This study

In this study, we investigated landslides in the northern half of the Taihang Mountains in China using optical remote sensing images and human–computer interactive visual interpretation methods and created a corresponding landslide database. Comparing the scope and number of landslide inventories with the existing landslide inventories in the Taihang Mountains region mentioned above, it can be found that the present study covers the entire northern half of the Taihang Mountains, with a total area of about 33,000 km^2, and 8349 landslides have been deciphered. This is the most extensive and data-rich landslide inventory in the database study of landslides in the Taihang Mountains region so far.

5.2. Strengths and Limitations of the Research Methodology

In terms of research methods, optical remote sensing has the ability to work in all-weather conditions and is not limited by cloud interference. In cloudy areas, optical remote sensing can penetrate the clouds and obtain high-resolution images of the ground surface. However, optical remote sensing also has some limitations. Optical remote sensing requires extremely high light conditions and cannot be detected at night or on cloudy or rainy days. The human–computer interactive visual interpretation method used in this study can make full use of human visual perception and cognitive ability to subjectively interpret and analyze remote sensing images. This helps to extract more useful landslide information from remotely sensed images. Second, human–computer interactive visual interpretation can reduce the possibility of human error. The influence of personal bias and misinterpretation on the results can be reduced through multi-person co-operation and mutual verification. However, human–computer interactive visual interpretation has some limitations. First, it requires specialists to operate and analyze, which may increase the cost of manpower and time. Second, the results of human–computer interactive visual interpretation may be affected by human factors, such as the operator's experience and skills. In addition, this study did not incorporate techniques such as InSAR and LiDAR, and there may be some slippery slopes that were missed during the investigation.

5.3. Future Prospects

The northern half of the Taihang Mountains has long been an area prone to landslides, which can lead to the destruction of houses, roads, and other infrastructure, resulting in casualties. Landslides can also cause damage to rivers, lakes, and other water sources, affecting the water supply and having a serious impact on the people living in the area. The inventory of landslides in the northern half of the Taihang Mountains that was eventually obtained in this study can provide detailed information on the magnitude and geographic location of landslides for stakeholders such as discussion policy makers, urban planners, environmentalists, and local communities. This will help in effective local risk prevention and management. For example, by setting up landslide monitoring instruments in advance based on the landslides marked in the inventory, this can reduce casualties and property damage. Predictive modelling based on databases and applying advanced techniques such

as machine learning to assess landslide risk is also possible. Alternatively, geological data can be combined with climate change projections for interdisciplinary research. We will also develop digital platforms in the near future to facilitate access to and the use of these landslide data.

6. Conclusions

The object of this study is the northern half of the Taihang Mountain Range, which covers a total area of about 33,000 km^2. By using multi-temporal high-resolution remote sensing images provided by the Google Earth platform, the landslide cataloging work in the study area was completed by the method of human–computer interactive visual interpretation. The results showed that the total number of landslides in the northern half of the Taihang Mountains was 8349, with a total area of 151.61 km^2, of which the largest landslide had an area of 2.83 km^2 and the smallest landslide had an area of 5.95 m^2. The areas with more intensive landslide development are mainly in the Taihang Mountains area in Xinzhou City and Taiyuan City, Shanxi Province. Compared with the results of previous studies, the database of landslides in the northern half of the Taihang Mountains obtained in this study is more complete. The multi-temporal high-resolution remote sensing imagery used allows for the acquisition of surface information at different points in time in the same area, leading to more comprehensive and accurate landslide extraction. The human–computer interactive visual interpretation technique is used in the study. This technique, combined with the interpreter's own professional experience and judgement, can more accurately identify some subtle features, thus improving the accuracy of landslide identification. The inventory of landslides in the northern half of the Taihang Mountains obtained in this study can be used to develop targeted ecological restoration strategies, such as planting anti-slip plants and installing slope protection projects. Urban planners can develop land use plans based on the landslide database to ensure that urban construction takes place in areas with low landslide risk. By analyzing this landslide inventory, it is also possible to determine which areas are most likely to require emergency resources in the event of a landslide, so that resources can be allocated and deployed in advance. In the future, we can also conduct more research based on this landslide database, including spatial distribution and landslide evaluation in the northern half of the Taihang Mountains, to provide a scientific basis for landslide prevention in the region.

Author Contributions: Conceptualization, C.X. and W.Y.; methodology, X.Z.; validation, C.X.; formal analysis, X.Z.; data curation, X.Z., L.F. and L.L.; writing—original draft preparation, X.Z.; writing—review and editing, X.Z. and C.X.; visualization, X.Z.; supervision, C.X. and W.Y.; project administration, C.X. All authors have read and agreed to the published version of the manuscript.

Funding: This research was funded by the National Nonprofit Fundamental Research Grant of China, grant number 2023-JBKY-57 and the Beijing Science and Technology Plan Project, grant number Z231100003823035.

Data Availability Statement: The datasets used and/or analyzed during the current study are available from the corresponding author on reasonable request.

Acknowledgments: We are grateful to the anonymous reviewers for their constructive comments and suggestions that improved the quality of the manuscript.

Conflicts of Interest: The authors declare no conflicts of interest.

References

1. Tiranti, D.; Cremonini, R. Editorial: Landslide hazard in a changing environment. *Front. Earth Sci.* **2019**, *7*, 3. [CrossRef]
2. Xu, C.; Gorum, T.; Tanyas, H. Editorial: Application of remote sensing and GIS in earthquake-triggered landslides. *Front. Earth Sci.* **2022**, *10*, 964753. [CrossRef]
3. Herrera, G.; Mateos, R.M.; García-Davalillo, J.C.; Grandjean, G.; Poyiadji, E.; Maftei, R.; Filipciuc, T.-C.; Jemec Auflič, M.; Jež, J.; Podolszki, L.; et al. Landslide databases in the geological surveys of europe. *Landslides* **2018**, *15*, 359–379. [CrossRef]
4. Gatto, A.; Clò, S.; Martellozzo, F.; Segoni, S. Tracking a Decade of Hydrogeological Emergencies in Italian Municipalities. *Data* **2023**, *8*, 151. [CrossRef]

5. Damm, B.; Klose, M. The landslide database for Germany: Closing the gap at national level. *Geomorphology* **2015**, *249*, 82–93. [CrossRef]
6. Cui, Y.; Yang, W.; Xu, C.; Wu, S. Distribution of ancient landslides and landslide hazard assessment in the Western Himalayan Syntaxis area. *Front. Earth Sci.* **2023**, *11*, 1135018. [CrossRef]
7. Mirus, B.B.; Jones, E.S.; Baum, R.L.; Godt, J.W.; Slaughter, S.; Crawford, M.M.; Lancaster, J.; Stanley, T.; Kirschbaum, D.B.; Burns, W.J.; et al. Landslides across the USA: Occurrence, susceptibility, and data limitations. *Landslides* **2020**, *17*, 2271–2285. [CrossRef]
8. Van Den Eeckhaut, M.; Hervás, J. State of the art of national landslide databases in Europe and their potential for assessing landslide susceptibility, hazard and risk. *Geomorphology* **2012**, *139–140*, 545–558. [CrossRef]
9. Guzzetti, F. Landslide fatalities and the evaluation of landslide risk in Italy. *Eng. Geol.* **2000**, *58*, 89–107. [CrossRef]
10. Rosser, B.; Dellow, S.; Haubrock, S.; Glassey, P. New Zealand's national landslide database. *Landslides* **2017**, *14*, 1949–1959. [CrossRef]
11. Cui, Y.; Bao, P.; Xu, C.; Ma, S.; Zheng, J.; Fu, G. Landslides triggered by the 6 September 2018 Mw 6.6 Hokkaido, Japan: An updated inventory and retrospective hazard assessment. *Earth Sci. Inform.* **2021**, *14*, 247–258. [CrossRef]
12. Xu, Y.; Allen, M.B.; Zhang, W.; Li, W.; He, H. Landslide characteristics in the Loess Plateau, northern China. *Geomorphology* **2020**, *359*, 107150. [CrossRef]
13. Zhao, S.; Dai, F.; Deng, J.; Wen, H.; Li, H.; Chen, F. Insights into landslide development and susceptibility in extremely complex alpine geoenvironments along the western Sichuan–Tibet Engineering Corridor, China. *Catena* **2023**, *227*, 107105. [CrossRef]
14. Zhang, X.; Li, L.; Xu, C. Large-scale landslide inventory and their mobility in Lvliang City, Shanxi Province, China. *Nat. Hazards Res.* **2022**, *2*, 111–120. [CrossRef]
15. Li, L.; Xu, C.; Yang, Z.; Zhang, Z.; Lv, M. An Inventory of large-scale landslides in Baoji City, Shaanxi Province, China. *Data* **2022**, *7*, 114. [CrossRef]
16. Wang, M.; Li, J.; Zhang, Y. Study on the outstanding universal value in geological heritage resources in the northern part of Taihang Mountain world heritage priority potential area. *Nat. Herit.* **2020**, *5*, 52–60.
17. Lin, L. Geomorphic Features of the Greater Khingan Mountains-Taihang Mountains and Its Tectonic Implications. Ph.D. Thesis, Institute of Geology, China Earthquake Administration, Beijing, China, 2022.
18. Wang, H.; LI, J.; Wu, T. Characteristics and genesis of geoheritage resources of Taihang Mountain. *Acta Sci. Nat. Univ. Pekin.* **2018**, *54*, 546–554.
19. Tian, Y.; Xu, C.; Xu, X.; Chen, J. Detailed inventory mapping and spatial analyses to landslides induced by the 2013 Ms 6.6 Minxian earthquake of China. *J. Earth Sci.* **2016**, *27*, 1016–1026. [CrossRef]
20. Zhang, P.; Xu, C.; Ma, S.; Shao, X.; Tian, Y.; Wen, B. Automatic extraction of seismic landslides in large areas with complex environments based on deep learning: An example of the 2018 Iburi Earthquake, Japan. *Remote Sens.* **2020**, *12*, 3992. [CrossRef]
21. Guzzetti, F.; Mondini, A.C.; Cardinali, M.; Fiorucci, F.; Santangelo, M.; Chang, K.-T. Landslide inventory maps: New tools for an old problem. *Earth-Sci. Rev.* **2012**, *112*, 42–66. [CrossRef]
22. Qin, Q. The problem and approach in the Auto-interpretation of remote sensing imagery. *Sci. Surv. Mapp.* **2000**, *25*, 21–24+21.
23. Mantovani, F.; Soeters, R.; Van Westen, C. Remote sensing techniques for landslide studies and hazard zonation in Europe. *Geomorphology* **1996**, *15*, 213–225. [CrossRef]
24. Guo, Z.; Nie, H.; Yang, L.; Tu, J.; He, P.; Tong, L. Ancient landslide identification and characteristics using remote sensing along Eastern Edge of the Heqing Basin. *Geoscience* **2014**, *28*, 1068–1076.
25. Lillesand, T.; Kiefer, R.W.; Chipman, J. *Remote Sensing and Image Interpretation*; John Wiley & Sons: Hoboken, NJ, USA, 2015.
26. Xu, C.; Wang, S.; Xu, X.; Zhang, H.; Tian, Y.; Ma, S.; Fang, L.; Lu, R.; Chen, L.; Tan, X. A panorama of landslides triggered by the 8 August 2017 Jiuzhaigou, Sichuan Ms 7.0 earthquake. *Seismol. Geol.* **2018**, *40*, 232–260.
27. Geertsema, M.; Schwab, J.; Blais-Stevens, A.; Sakals, M. Landslides impacting linear infrastructure in west central British Columbia. *Nat. Hazards* **2009**, *48*, 59–72. [CrossRef]
28. Messerli, B.; Ives, J.D. *Mountains of the World: A Global Priority*; Parthenon Publishing Group: New York, NY, USA, 1997.
29. Froude, M.J.; Petley, D.N. Global fatal landslide occurrence from 2004 to 2016. *Nat. Hazards Earth Syst. Sci.* **2018**, *18*, 2161–2181. [CrossRef]
30. Trigila, A.; Iadanza, C.; Spizzichino, D. Quality assessment of the Italian landslide inventory using GIS processing. *Landslides* **2010**, *7*, 455–470. [CrossRef]
31. Ma, R.; Lyu, Y.; Chen, T.; Zhang, Q. Preliminary risk assessment of geological disasters in Qinglong Gorge Scenic Area of Taihang Mountain with GIS based on analytic hierarchy process and logistic regression model. *Sustainability* **2023**, *15*, 15752. [CrossRef]
32. Wu, J.; Ma, C.; Yang, W.; Lyu, L.; Miao, L. Recent expansion of talus slopes in the northern Taihang Mountain Range, China: An example from the Xiaowutai Region. *Landslides* **2021**, *18*, 3027–3040. [CrossRef]
33. Li, Y.; Ma, C.; Wang, Y. Landslides and debris flows caused by an extreme rainstorm on 21 July 2012 in mountains near Beijing, China. *Bull. Eng. Geol. Environ.* **2019**, *78*, 1265–1280. [CrossRef]
34. Wei, A.; Yu, K.; Dai, F.; Gu, F.; Zhang, W.; Liu, Y. Application of Tree-Based ensemble models to landslide susceptibility mapping: A comparative study. *Sustainability* **2022**, *14*, 6330. [CrossRef]
35. Zhang, W.; Zhao, J.; Shen, R.; Liu, Y.; Gu, F. Analysis of geological hazard types and distribution pattern in Xindu District. *Geosci. Remote Sens.* **2023**, *6*, 1–7.

36. Gao, W. Main Mechanism and Fatalness Evaluation of Rockfall in Juma River Region, the North of Taihang Mountain. Master's Thesis, China University of Geosciences (Beijing), Beijing, China, 2009.
37. Lv, Y.; Chen, T.; Wang, Z.; Zhao, J.; Zhan, J.; Liu, X. Study on the development characteristics and genetic patterns of collapses in the Taihang Mountain Grand Canyon, China. *J. Eng. Geol.* **2022**, *30*, 1304–1315.